# Upper Crustal Structure across the Japan Trench at 40°N

Tôhoku Geophys. Journ. (Sci. Rep. Tôhoku Univ., Ser. 5), Vol. 32, Nos. 3, 4, pp. 37-54, 1990 37

# *Upper Crustal Structure across the Japan Trench at 40°N*

AZUSA NISHIZAWA

Observation Center for Prediction of Earthquakes and Volcanic Eruptions, Faculty of Science, Tohoku University, Sendai 980

KIYOSHI SUYEHIRO

Ocean Research Institute, University of Tokyo, Tokyo 164

(Received July 7, 1989)

*Abstract*: An airgun and OBS (Ocean Bottom Seismograph) seismic refraction experiment was carried out to investigate the lateral change in crustal structure in detail across the northern part of the Japan Trench in 1981. We analyzed the data by a 2-dimensional ray tracing method and determined wavespeed-depth models for the trench region.

Two main conclusions are drawn from this study and previously published results; (1) seismic wavespeed of sediments beneath the inner trench slope seems to vary along the Japan Trench axis apparently not directly related to the Pacific plate subduction; (2) wavespeed in layer 3 beneath the outer trench slope is lower than that of the typical oceanic basin possibly due to serpentinization in the layer caused by bending of the plate.

## 1. Introduction

The Japan Trench region is well known as a typical subduction area (Fig. 1) where many geophysical researches have been made. Especially, in the region of 40°N of the Japan Trench, a number of reflection and refraction experiments were carried out in order to understand subduction tectonics (*e.g.*, Ludwig *et al.*, 1966; Murauchi and Ludwig, 1980; Nagumo *et al.*, 1980; Nasu *et al.*, 1980; Matsuzawa *et al.*, 1980; Asano *et al.*, 1981; Tamano *et al.*, 1981). The transition of crustal structure across the trench became evident from these profilings. For example, multichannel reflection experiments showed clear signals from the subducting oceanic layer 2 up to 40-60 km landward from the trench axis (Tamano *et al.*, 1981). Results from several refraction experiments show the Moho depth becomes deeper from 12 km at the oceanic basin (Murauchi and Ludwig, 1980) to 25 km beneath the continental slope at the water depth of about 1,500 m (Asano *et al.*, 1981).

Recently, seismic refraction experiments by using repetitive controlled seismic sources and Ocean Bottom Seismographs (OBSs) as low noise, fixed point receivers have been carried out, which are effective to study more detailed crustal structure. In 1981, we made a refraction experiment at the northern part of the Japan Trench. An airgun and explosive sources were shot around 40°N of the Japan Trench. The airgun data from the profiles along 3,000 m isobath were analyzed by Suyehiro *et al.* (1985). The

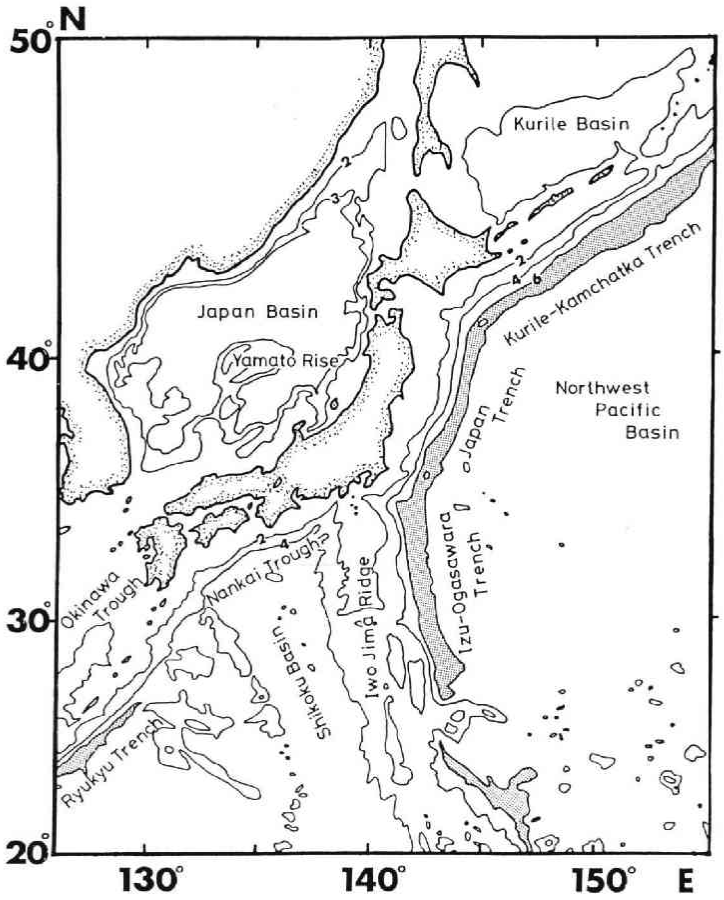


Fig. 1 Map of the major bathymetric features of the Japan region.

mean structure obtained by them indicated that there exist 1.9 and 4.8 km/s wavespeed materials with 1.5 and 3.5 km thicknesses, respectively, and that a layer with a P wavespeed of 6.0 km/s underlies them. The Moho depth is about 18 km obtained from PmP arrivals. Preliminary results from the explosion experiment were presented by Kanazawa *et al.* (1985). These and former results compiled by Suyehiro *et al.* (1986) are shown in Fig. 2.

In this paper, we analyze the data obtained from the profiles nearly perpendicular to the trench axis in the 1981 experiment in order to examine lateral heterogeneity of the crustal structure in the inner trench region.

## 2. Experiment and Data Reduction

The positions of OBSs in the 1981 experiment are shown in Fig. 3 and Table 1. Only T9 was tethered type and the others were pop-up type OBSs. These instruments had a vertical and a horizontal sensor and signals were recorded on an analog cassette tape

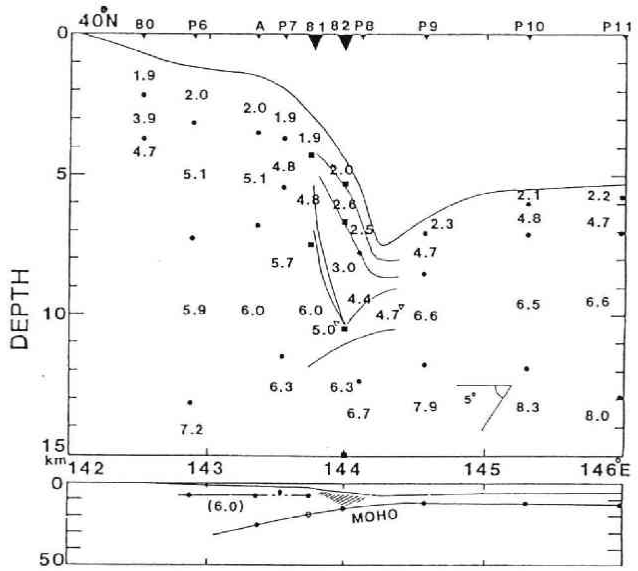


Fig. 2 P wavespeed structure at the Japan Trench off Sanriku, 40°N given by Suyehiro *et al.* (1986). The upper figure contains results from refraction proflings using two-ship, sonobuoy, or OBS technique and from multi-channel reflection profilings. Bottom figure shows the Moho depth, low wavespeed prism (hatched area) and presence of material with continental upper crustal wavespeed.

Table 1. Ocean Bottom Seismograph Stations

| Instrument | Latitude (°N) | Longitude (°E) | Depth (m) |
|---|---|---|---|
| P1 | 39.75 | 142.75 | 1190 |
| P4 | 40.12 | 143.37 | 1360 |
| P6 | 39.45 | 143.63 | 3340 |
| P7 | 39.75 | 143.66 | 3210 |
| P8 | 40.03 | 143.70 | 2670 |
| T9 | 40.47 | 143.76 | 3280 |
| P10 | 39.87 | 144.01 | 4370 |
| P12 | 39.90 | 144.63 | 6055 |

(Yamada, 1980). As an artificial seismic source, an airgun (Bolt type, 9 liter, 100 kg/cm$^2$) was shot every 150-200 m interval.

In the four profiles crossing P1, the airgun was shot in different directions to investigate azimuthal variation of the crustal structure. A split profile and a fan shooting were carried out for P12 and, in this paper, we analyzed the split profile to determine the wavespeed-depth function. Almost all the profiles were split ones of which directions were not parallel to the isodepths.

The OBS's records were digitally processed to obtain record sections. Unfortunate-

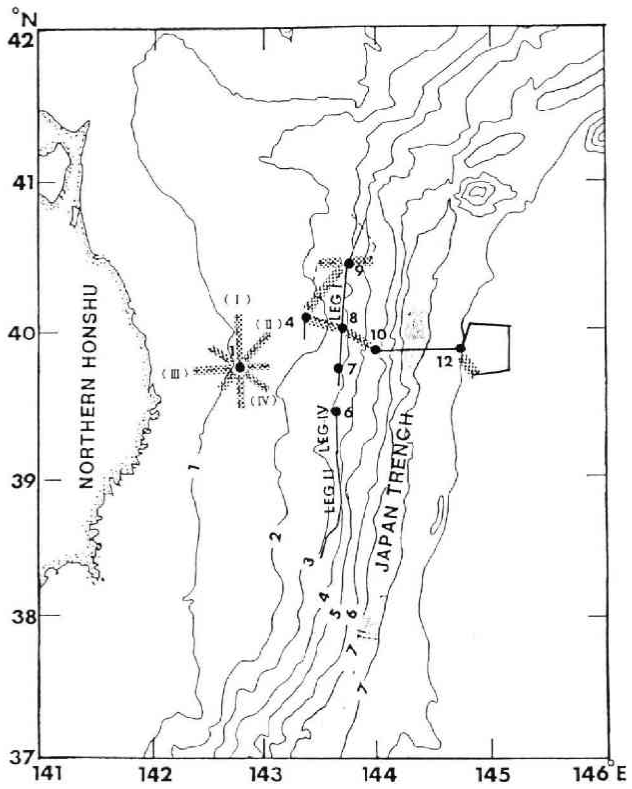


Fig. 3 Locations of OBSs (solid circles) and refraction lines in 1981 experiment study in relation to the local bathymetry. Thin solid lines along 3,000 m isobath represent the profiles analyzed by Suyehiro *et al.* (1986) and the profiles with shadowed liens are discussed in this study.

ly, we could not obtain accurate absolute ship position during the experiment owing to the malfunction of Loran C and we determined the epicentral distances only by water wave travel times. When the water depth of the OBS is shallow, it is difficult to pick water wave arrivals because many multiples appear in the seismograms. In such a case, the error of the epicentral distance can amount to 1 km over the range of 20 km, which causes an error of more than 5% in P wavespeed (in the worst case of P1).

## 3. Analyses

We first applied a conventional apparent wavespeed-intercept time method by assuming a sloped and layered structure and obtained an initial wavespeed model. In this step, we used observed travel time data. Next, in order to include lateral heterogeneity in the wavespeed model, the model was refined by using 2-dimensional ray tracing program SEISOBS for OBS receivers (Hirata and Shinjo, 1986), which is a modified version of SEIS83 (Červený and Pšenčík, 1983). In the second step, we examined amplitude variation with epicentral distances. Following criteria were used

in constructing a wavespeed model by the ray tracing method : (1) a simpler model will be chosen, *e.g.* with a smaller number of layers ; (2) wavespeed discontinuities are not brought in unless required ; (3) each layer in the model is laterally homogeneous ; (4) if the heterogenities are unavoidable, such heterogeneities tend to exist in the shallower part of the model. Variation of sea floor topography produces important effects on the record sections. In our model, we used the results of the single-channel reflection profiling conducted during the same OBS experiments.

In the case of profile I for P1 which had relatively flat seafloor topography, we could transform the record sections in the travel time and distance domain to the intercept time and ray-parameter domain by slant stack procedure. This method is objective and no information is lost during the operation. To eliminate most of the spatial aliasing,

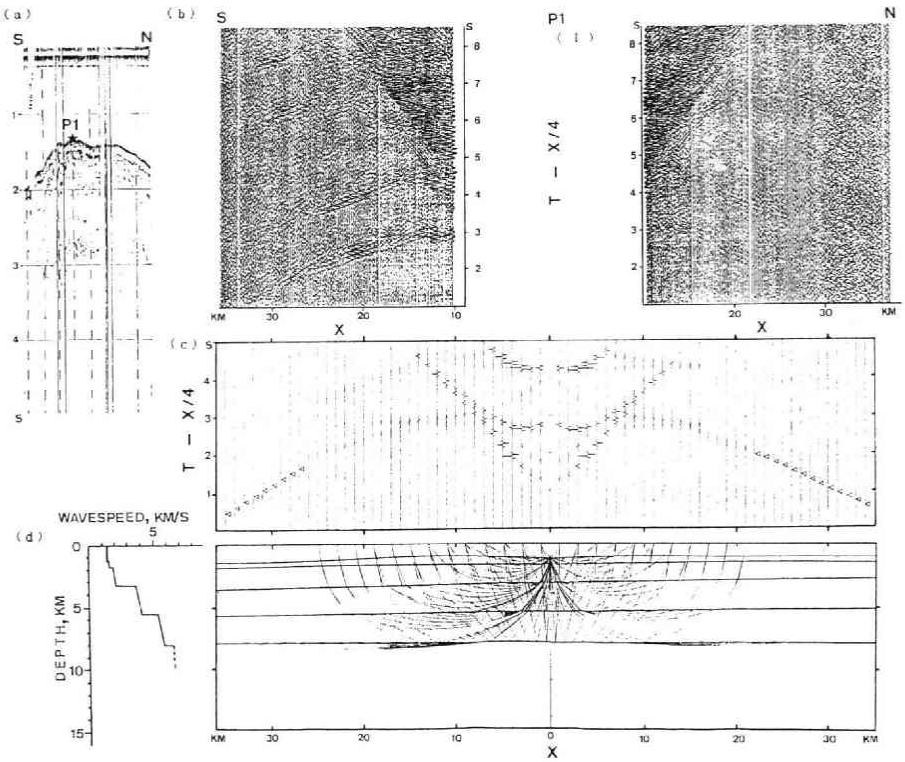


Fig. 4 (a) Singe-channel reflection records obtained at the same time of the refraction experiment. (b) Observed vertical component seismograms for profile I of P1. The data are bandpass filtered (5-25 Hz), and a gain factor proportional to distance squared has been used to enhance the distant seismograms. (c) Synthetic seismograms calculated by the asymptotic ray theoretical approach of Červený and Pšenčík (1983) for the P wavespeed model given in (d). A gain factor proportional to distance squared has been applied. Arrivals with very small amplitudes are shown by open triangles. (d) right : wavespeed model and ray paths obtained using tau-sum inversion and forward ray tracing. The top layer is water. left : wavespeed-depth function beneath the OBS in the laterally heterogeneous model on the right.

semblance windowing was applied to the slant stack (Stoffa *et al.*, 1981). We picked the postcritical reflection and refraction signals. After that, we inverted these signals to 1-dimensional wavespeed-depth function by using tau-sum inversion method (Diebold *et al.*, 1981; Diebold and Stoffa, 1981). Then we improved the model by the 2-D ray tracing.

## 4. Results

We show the results of each profile from continental side to oceanic side across the trench. We excluded the data obtained at P10 because of the poor records.

### *4.1. Inner Trench Slope*

P1 was positioned at the shallowest point on the continental slope (water depth of 1,190 m) in this experiment. We shot four profiles for P1. For relatively flat topography of the profile I (Fig. 4(a)) of which direction was nearly parallel to the trench axis, we calculated tau-$p$ section of the data by a slant stack method (Fig. 5). Bounded area in Fig. 5(a) corresponds to the region where the refractions and postcritical reflections exist at some intensity level. We picked these signals and inverted them to the limits of the wavespeed-depth function. The results show a constant wavespeed gradient up to a depth of 7 km.

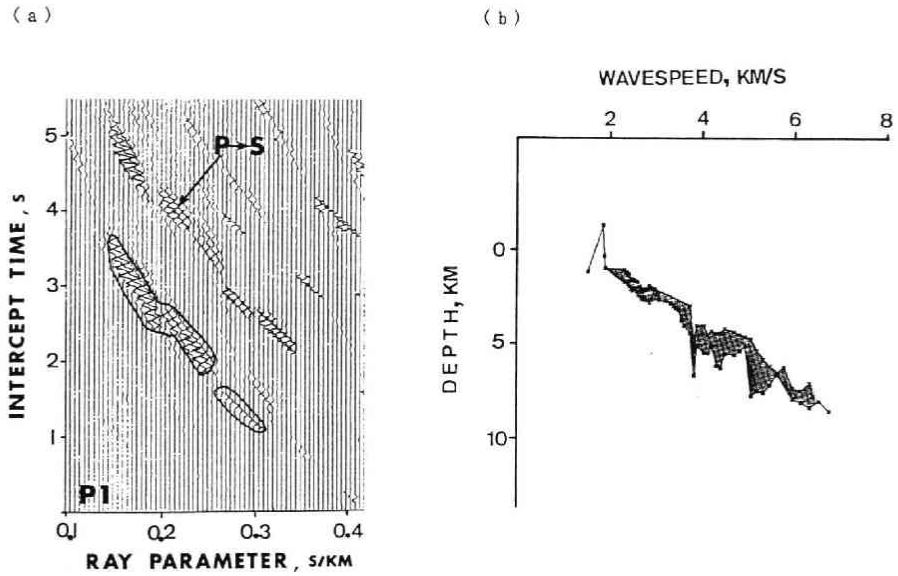


Fig. 5 (a) Tau-p representation of the vertical seismograms obtained from the profile I for OBS P1. The bounds on the tau-p function were used to derive the wavespeed-depth functions. (b) The results from travel time inversion of the tau-p data. The inversions were obtained using tau-sum method of Diebold and Stoffa (1981). The upper and lower limits of the wavespeed-depth paths are derived from error estimated for each tau point. This results is used to construct a starting model for the forward computation of ray tracing.

However, the record section (Fig. 4(b)) shows clear P to S converted signals about 1.5 s after the first arrivals, which suggests there exists a wavespeed boundary just beneath the OBS P1. Adding this information to the result of the inversion, we constructed a 2-dimensional wavespeed model (Fig. 4(d)) which fits to the observed record section within an accuracy of 0.1 s. In the model the upper two layers are estimated to be unconsolidated sediments taking their average P wavespeeds of 1.6 and 2.0 km/s into consideration. Consolidated sediments with a P wavespeed of 3.5 km/s at the top underlie the unconsolidated layers. P to S converted waves were generated at the boundary between the unconsolidated and consolidated layers and the P to S wavespeed ratio of the top two layers is estimated to be 2.4. The third layer has P wavespeeds of 3.5-4.8 km/s and thickness of 2.5 km. Average P wavespeed and thickness of the fourth layer are 5.5

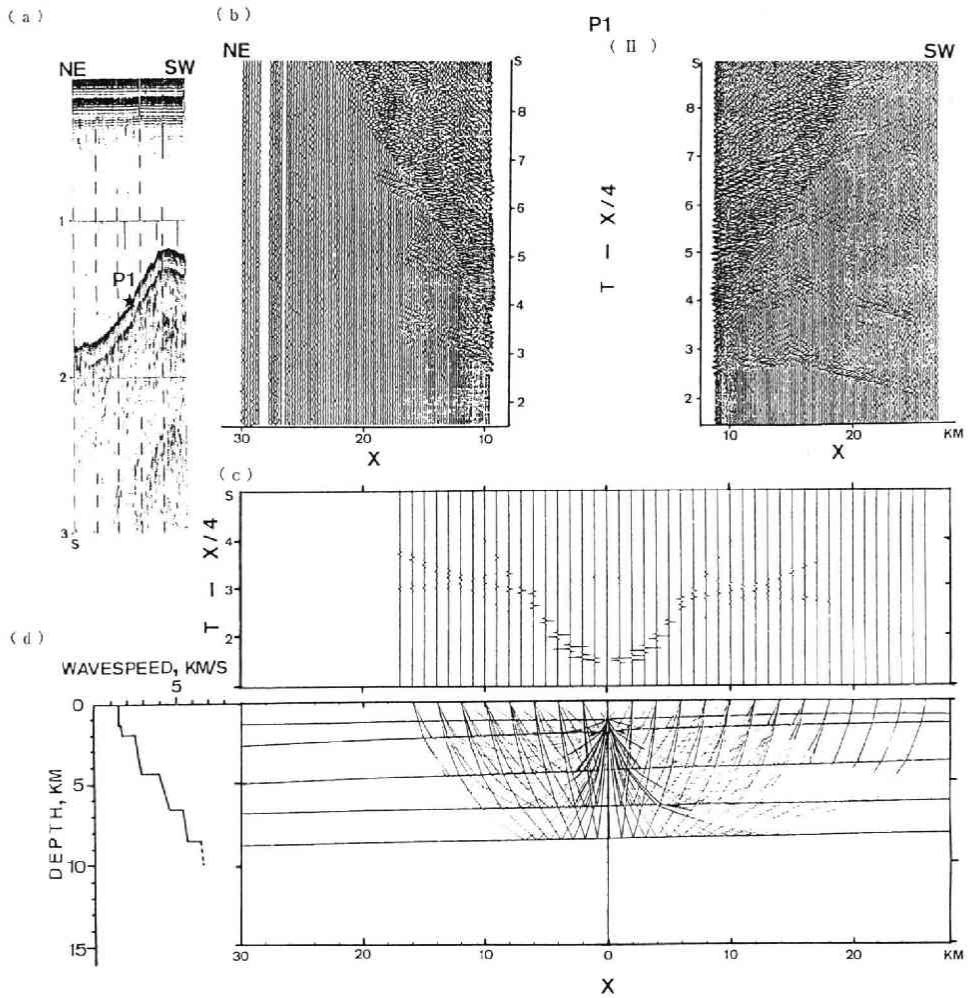


Fig. 6 Same as Fig. 4 but for the profile II of P1.

km/s and 2.5 km. The wavespeed of the lowermost layer is less accurate because of the weak signals from the layer.

Travel times of the signals from the second sedimentary layer beneath the profile II (Fig. 6(b)) indicate higher wavespeeds (2.5-2.8 km/s) than those of the profile I. We could not obtain the refracted arrivals with enough amplitude over the distance of 18 km in the synthetics of northeastern part of the profile (Fig. 6(c)), which corresponds to the observation (Fig. 6(b)). Since the record section for the profile III has the smallest epicentral distances of the four profiles for P1, we could analyze the shallower part of the crustal structure more accurately along this profile. The model is almost the same as that of the profile I rather than that of the profile II (Fig. 7). Although the profile IV is a single

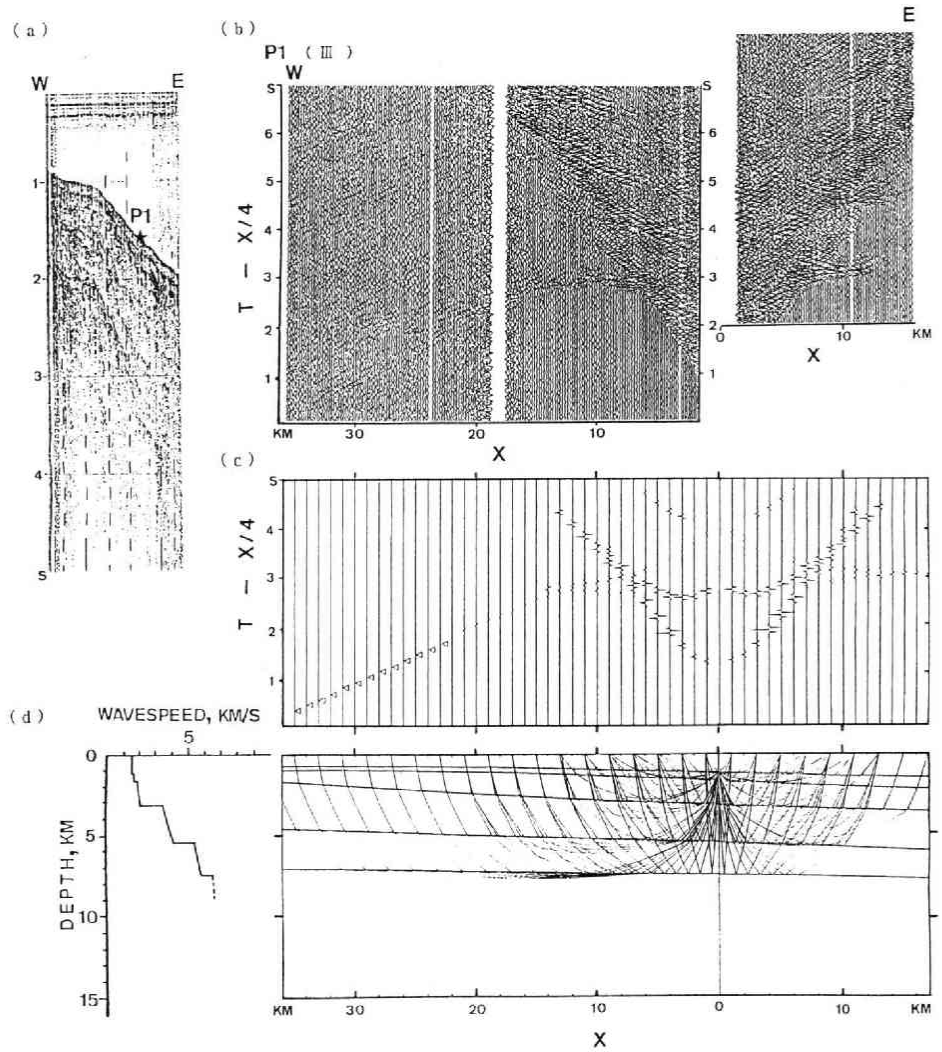


Fig. 7 Same as Fig. 4 but for the profile III of P1.

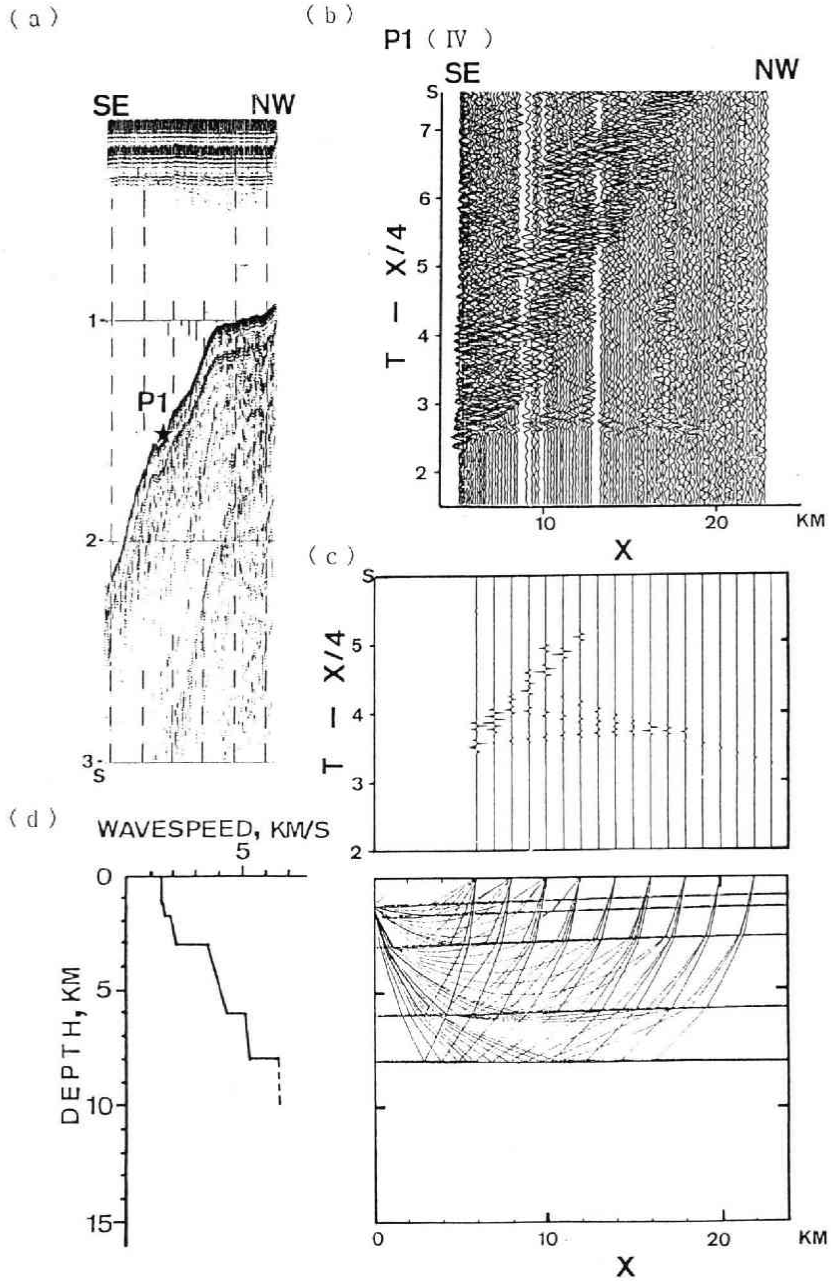


Fig. 8 Same as Fig. 4 but for the profile IV of P1.

profile which means a one sided profile, the record section is explained by almost the same wavespeed model as the profile I (Fig. 8).

Seismic reflection signals obtained by the single-channel hydrophone streamer are shown from OBS P4 to P10 in Fig. 9. The records are from the same airgun shots of the refraction experiment. We set P4 at the continental slope with a water depth of 1,360 m. The direction of the profile varied at P4. The water depth increases towards the trench from P4 to P10.

The wavespeed model for P4 (Fig. 10) has six layers to explain the amplitude variation with distance. Since the water depth increases with the epicentral distance on both sides of the profile, the apparent P wavespeeds at the distance of 10 km indicate higher than 5 km/s.

OBSs P8 and T9 were deployed along the isobath of 3,000 m. We processed the data of the airgun profiles of which directions were perpendicular to the trench axis. A single

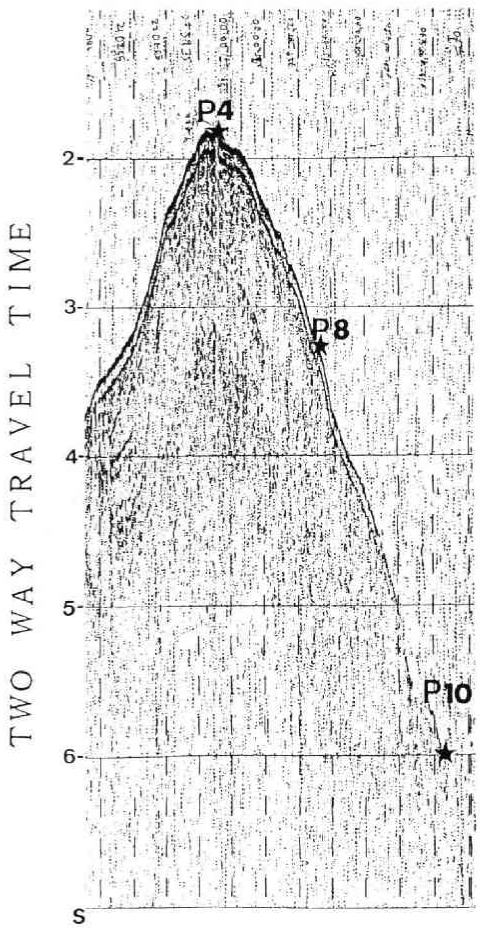


Fig. 9 Reflection records from P4 to P10. This is the single-channel hydrophone streamer output by the same airgun shots of the refraction experiment.

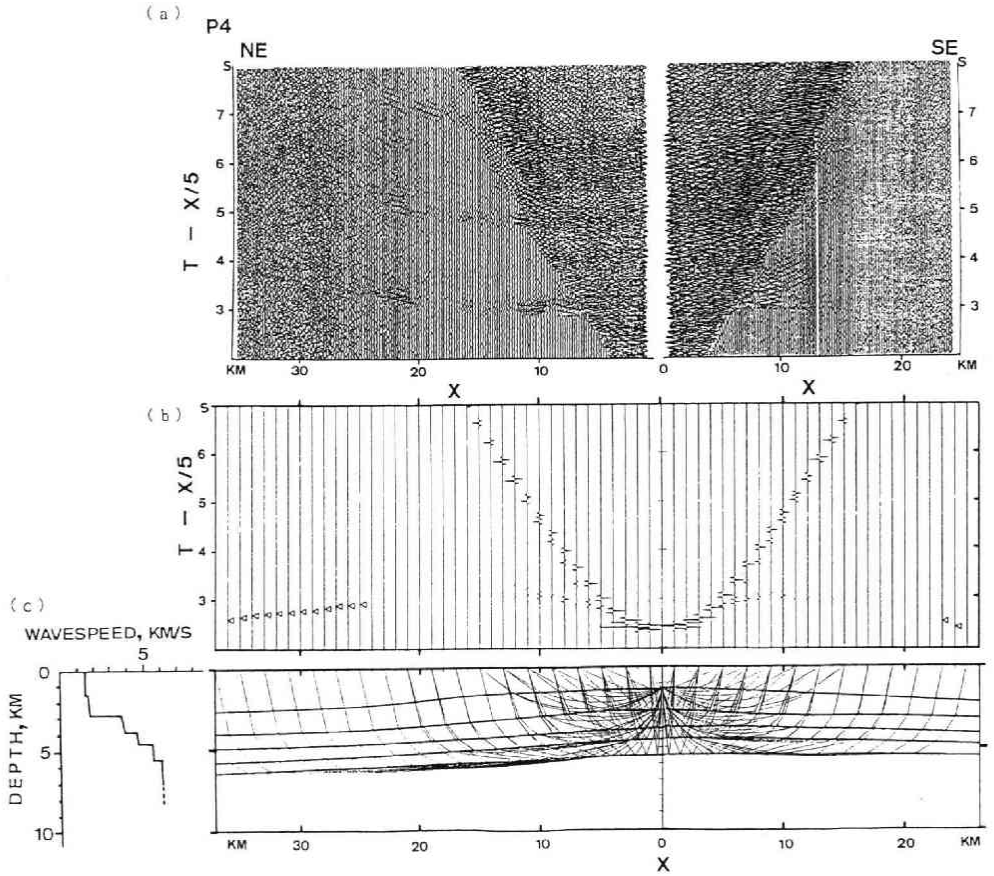


Fig. 10 (a) Observed vertical component seismograms for P4. The data are bandpass filtered (5-25 Hz), and a gain factor proportional to distance squared has been used to enhance the distant seismograms. (b) Synthetic seismograms calculated by the asymptotic ray theoretical approach of Červený and Pšenčík (1983) for the P wave-speed model given in (c). A gain factor proportional to distance squared has been applied. Arrivals with very small amplitudes are shown by open triangles. (c) right : wavespeed model and ray paths. The top layer is water. left : wavespeed-depth function beneath the OBS in the laterally heterogeneous model on the right.

profile for P8 was analyzed up to the epicentral distance of 30 km. Refraction signals at the epicentral distance more than 20 km are not seen owing to poor S/N ratio (Fig. 11(a)). Taking the water depth variation into consideration, the refraction signals around 10 km range indicate a wavespeed higher than 4 km/s. For T9, however, clear arrivals are identified at the range over 20 km (Fig. 12(a)). Apparent difference in the observed record sections between both sides of the profile can be attributed to the change in water depth. Although a slight wavespeed discontinuity at the depth of 5 km is modeled to explain the large amplitude near the epicentral distance of 10 km for P8, the average wavespeed-depth functions of the two OBSs are not different from one another.

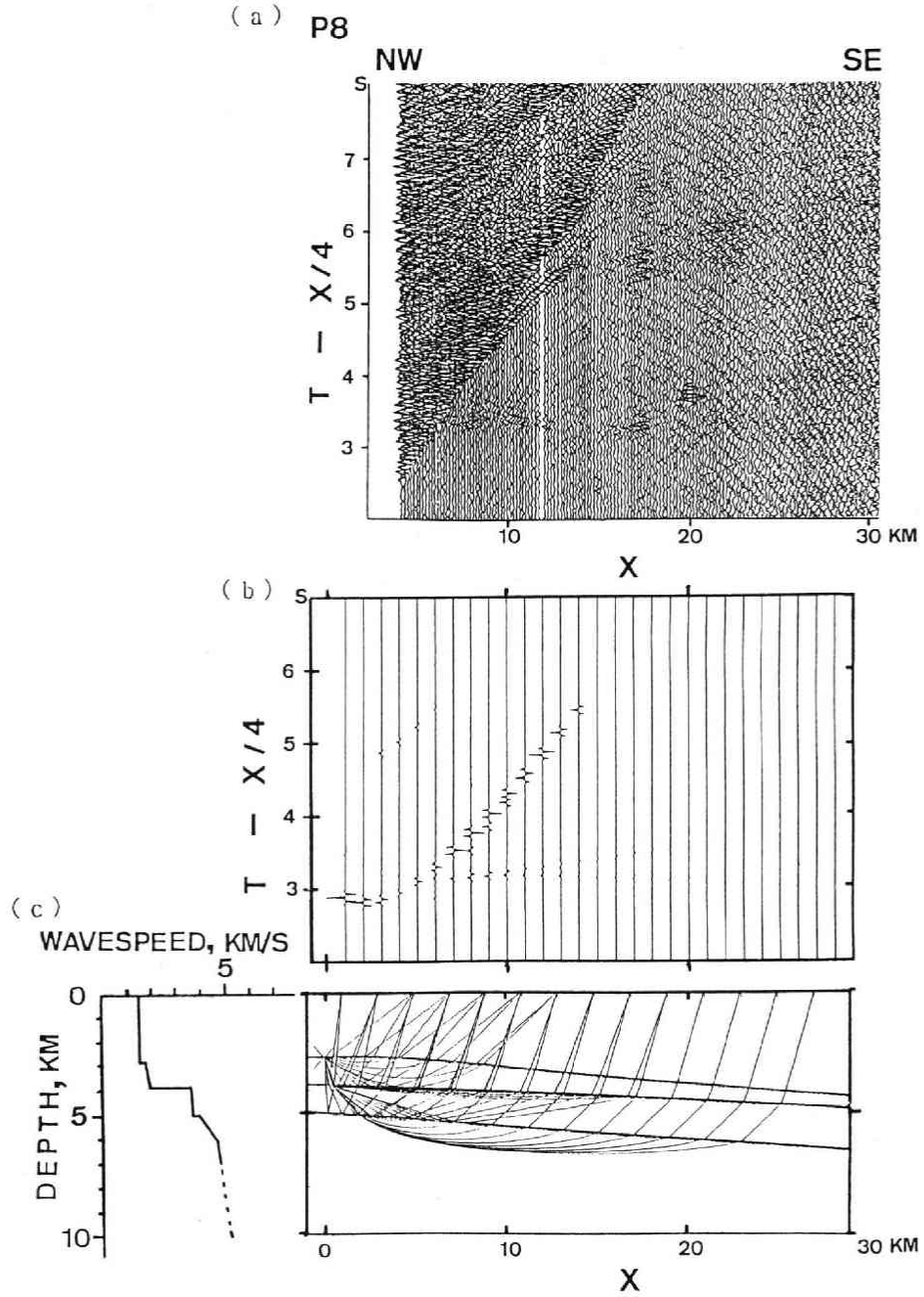


Fig. 11 Same as Fig 10 but for P8.

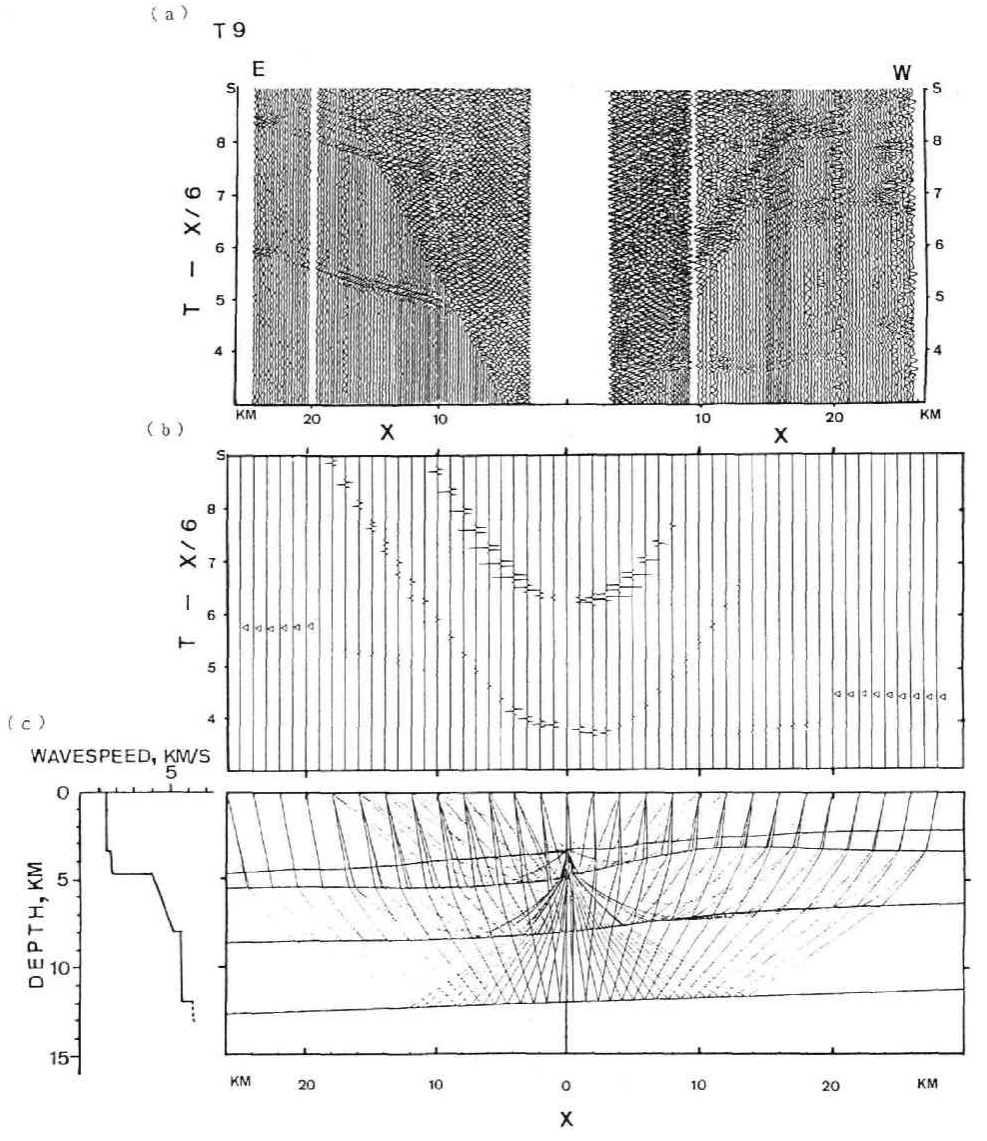


Fig. 12 Same as Fig. 10 but for T9.

### *4.2. Outer Trench Slope*

P12 was positioned at an outer trench slope (water depth of 6,055 m). We analyzed the longest single profile for P12 to determine the P wavespeed-depth function. The direction of the profile was parallel to the trench axis and the topography was almost flat. The wavespeed-depth function in Fig. 13(c) shows existence of the oceanic layer 2 with a large wavespeed gradient and oceanic layer 3 with a nearly constant wavespeed. However, the wavespeed of layer 3 (average 6.4 km/s) is lower than that of the typical

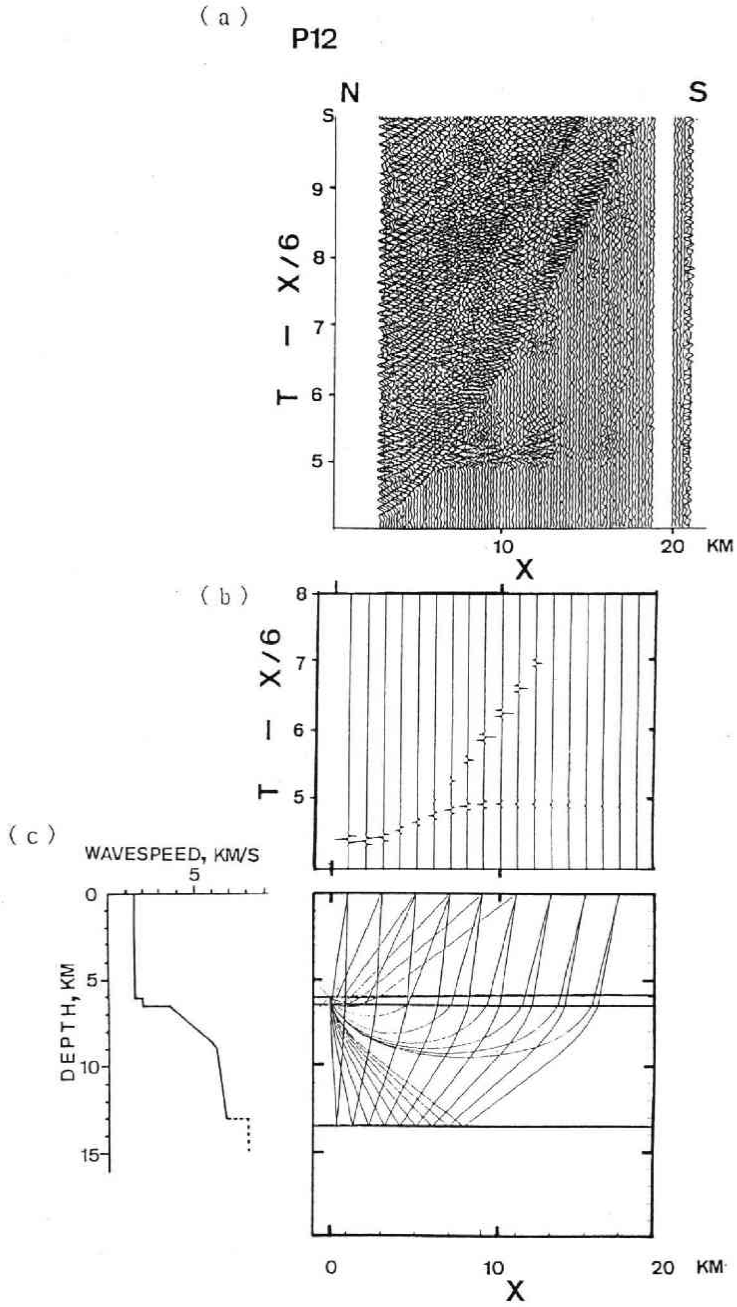


Fig. 13 Same as Fig. 10 but for P12.

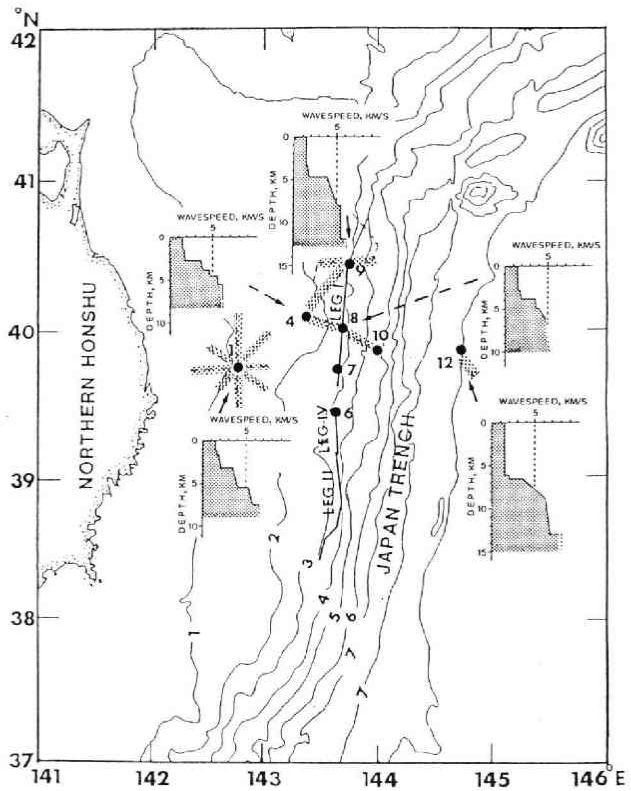


Fig. 14 The final model of the P wavespeed structure obtained in this experiment. The wavespeed-depth function at a point, say P1, is an average one beneath P1. The top layer is sea water.

oceanic crust (average 6.7 km/s).

## 5. Discussion and Conclusions

P wavespeed-depth functions obtained in this experiment are compiled in Fig. 14.

Four seismic wavespeed models for P1 are not different among them except for the shallower part of the profile II. Regrettably, we could not confirm the difference between the profile I and II, because it is within the error of inaccurate epicentral distances. Apparent disagreements between the record sections of the profile I, III and IV are mainly due to the topography along the profile.

The 250 km-long profile along the 3,000 m depth contour includes P8 and T9 and was analyzed by Suyehiro *et al.* (1986) (Fig. 2). Although their preliminary results show that a 4.8 km/s layer underlies the topmost sedimentary layer, this experiment rather suggests that there exists a layer with a wavespeed gradient (P wavespeed of 4.0 km/s at the depth of 4.8 km and 5.1 km/s at 8 km) which explains the observed amplitude data. They also pointed out a continental crust of 6 km/s layer exists along 3,000 m depth contour. Owing to the limit of the epicentral distance, however, we could not confirm

such layer except for weak signals from OBS T9.

Based on the previous multi-channel and drilling results (Honza, 1980), the P wavespeed models of the sediments beneath the inner continental slope indicate characters since Cretaceous. Our models for the upper sediments are divided into two groups; one includes P1 and P4 and the other contains P8 and T9. The model for P1 and P4 has a little thicker unconsolidated sediments (thickness of 1.8-2.4 km) than that for P8 and T9 (1.1-1.5 km). The P to S wavespeed ratios are about 2.4 for P1 and 3.8 for T9.

Along 3,000 m isobath in the middle Japan Trench at 37-38°N (off Fukushima), a 4.9-5.1 km/s layer exists just beneath the upper sedimentary layer with a P wavespeed of 1.9-2.2 km/s and a thickness of 2 km (Kaiho, 1988). This structure corresponds to our results for P8 and T9. On the other hand, 5-6 km thick materials with P wavespeeds of less than 5 km/s exist from the trench axis to about 50 km landward in the southern part of the Kurile Trench (Nishizawa and Suyehiro, 1986; Iwasaki *et al.*, 1989), where the same Pacific Plate is subducting. These differences suggest that the wavespeed structure beneath the inner slope of the Japan Trench is characterized not only by the subducting plate but also by the local tectonics landside.

The lower wavespeed of the oceanic layer 3 at P12 than that of the typical ocean was obtained. Ludwig *et al.* (1966) showed by the two-ship experiment that P wavespeeds of oceanic layer 3 at the region landward of the marginal swell (P8 and P9, in Fig. 2) were normal oceanic, that is, 6.6-6.7 km/s. However, the wavespeed of the oceanic layer 3 at 4,500 m depth of the inner trench slope (denoted by 82 in Fig. 2) was obtained to be 6.3 km/s by using airgun-OBS profiling (Suyehiro *et al.*, 1985). The average shot interval in the two-ship experiment was about 1 km compared to less than 200 m in our experiment, which causes less resolvable wavespeeds. Such a low P wavespeed of the layer 3 was also found beneath the trench axis region in the southern part of the Kurile Trench (Nishizawa and Suyehiro, 1986).

P12 was positioned at the outer trench slope where small normal faults due to the tensile field were observed by many reflection experiments. These normal faults are found to penetrate into the oceanic crust (Ludwig *et al.*, 1966), which seem to make its wavespeed lower. Moreover, supply of water through the fractures of the faults may increase serpentinization. P wavespeeds of 6.08-6.62 km/s measured for serpentinized peridotites at 1 kbar (Christensen, 1978) could explain the observed wavespeed. Furthermore this region corresponds to the seismically active zone (Hirata *et al.*, 1984, 1985; Kono *et al.*, 1988). These characteristics indicate that this region is deformed by the subduction of the oceanic plate.

By combining airgun-OBS profiling and 2-dimensional ray tracing method, we could obtain detailed crustal structures with lateral heterogeneity beneath the inner slope of the trench. In the outer trench slope, a lower P wavespeed of the oceanic layer 3 than that of the typical oceanic basin was estimated. We expect lower wavespeeds of the oceanic layer 3 will be found at other subduction zones by means of detailed crustal structure analyses. In the near future, we must investigate deeper structures around the trench region using a large airgun array to examine the effects on the trench materials

caused by the coupling of the landside tectonics and oceanic plate subduction.

*Acknowledgements*: The authors would like to thank Drs. H. Shimamura, T. Kanazawa, T. Iwasaki, N. Hirata and T. Urabe for their cooperation throughout this study. The authors wish to express their appreciation to Dr. A. Yamamoto, Dr. T. Matsuzawa, Mr. R. Ogawa and Mr. S. Ueno for their cooperation and assistance during the OBS deployment. The skilled ship maneuver and help by captain and the crew of M/S Ocean Discoverer of Fukada Salvage Co. Ltd. are acknowledged.

## References

Asano, S., T. Yamada, K. Suyehiro, T. Yoshii, Y. Misawa, and S. Iizuka, 1981: Crustal structure in a profile off the Pacific coast of northeastern Japan by the refraction method with ocean bottom seismometers, *J. Phys. Earth*, **29**, 267-281.

Červený, V., and I. Pšenčík, 1983: *Program package SEIS83*, Charles University, Prague.

Christensen, N.I., 1978: Ophiolites, seismic velocities and oceanic crustal structure, *Tectonophysics*, **47**, 131-157.

Diebold, J.B., and P.L. Stoffa, 1981: Venezuela Basin crustal structure, *J. Geophys. Res.*, **86**, 7901-7923.

Diebold, J.B., P.L. Stoffa, P. Boul, and M. Truchan, 1981: The travel time equation, tau-p mapping, and inversion of common mid point data, *Geophysics*, **46**, 238-254.

Hirata, N., and N. Shinjo, 1986: SEISOBS: Modified version of SEIS83 for ocean bottom seismograms, *Zisin, Ser. II*, **39**, 317-321 (in Japanese).

Hirata, N., T. Kanazawa, K. Suyehiro, and H. Shimamura, 1985: A seismicity gap beneath the inner wall of the Japan Trench as derived by OBS measurement, *Tectonophysics*, **112**, 193-209.

Hirata, N., T. Kanazawa, T. Iwasaki, K. Suyehiro, T. Urabe, and H. Shimamura, 1984: Microseismic activity beneath the Kuril Trench as derived by OBS observation, *Abstr. Ann. Seism. Soc. Japan*, **2**, p. 72 (in Japanese).

Honza, E., 1980: Pre-site survey of the Japan Trench transect, Deep Sea Drilling Project, in *Initial Reports of the Deep Sea Drilling Projects*, U.S. Government Printing Office, Washington, D.C., **56**, **57**, 489-503.

Iwasaki, T., H. Shiobara, A. Nishizawa, T. Kanazawa, K. Suyehiro, N. Hirata, T. Urabe, and H. Shimamura, 1989: A detailed subduction structure in the Kuril trench deduced from ocean bottom seismographic refraction studies, *Tectonophysics*, **165**, 315-336.

Kaiho, Y., 1988: Airgun-OBS profiling at the inner slope of the middle Japan Trench, *Mc. Sci. thesis, Chiba University*.

Kanazawa, T., K. Suyehiro, N. Hirata, T. Iwasaki, H. Shimamura, A. Nishizawa, and T. Urabe, 1985: Velocity structure beneath the inner slope of the Japan Trench, *Abstr. Ann. Seism. Soc. Japan*, **2**, p. 239 (in Japanese).

Kono, T., T. Matsuzawa, K. Nida, A. Hasegawa, A. Yamamoto, and A. Takagi, 1988: Earthquakes occurring near the Japan Trench axis off Tohoku, *Abstr. Ann. Seism. Soc. Japan*, **2**, p. 123 (in Japanese).

Ludwig, W.J., J.I. Ewing, M. Ewing, S. Murauchi, N. Den, S. Asano, H. Hotta, M. Hayakawa, T. Asanuma, K. Ichikawa, and I. Noguchi, 1966: Sediments and structure of Japan Trench, *J. Geophys. Res.*, **71**, 2121-2137.

Matsuzawa, A., T. Tamano, Y. Aoki, and T. Ikawa, 1980: Structure of the Japan Trench subduction zone from multichannel seismic reflection records, *Mar. Geol.*, **35**, 171-182.

Murauchi, S., and W.J. Ludwig, 1980: Crustal structure of the Japan Trench: The effects of subduction of oceanic crust, in *Initial Reports of the Deep Sea Drilling Projects*, U.S. Government Printing Office, Washington, D.C., **56**, **57**, 463-469.

Nagumo, S., J. Kasahara, and S. Koresawa, 1980: OBS airgun seismic refraction survey near sites 441 and 434 (J-1a), 438 and 439 (J-12), and proposed site J-2B: Legs 56 and 57, in *Initial Reports of the Deep Sea Drilling Projects*, U.S. Government Printing Office, Washington,

D.C., **56, 57**, 459-462.

Nagumo, S., J. Kasahara, S. Koresawa, and M. Kobayashi, 1980: Ocean bottom seismometer-airgun seismic refraction survey, in *Preliminary Report of the Hakuho Maru Cruise KH-77-1*, Ocean Research Institute, Univ. of Tokyo, 159-173.

Nasu, N., R. von Huene, Y. Ishikawa, M. Langseth, T. Bruns, and E. Honza, 1980: Interpretation of multichannel seismic reflection data, legs 56 and 57, Japan Trench transect, in *Initial Reports of the Deep Sea Drilling Projects*, U.S. Government Printing Office, Washington, D.C., **56, 57**, 489-503.

Nishizawa, A., and K. Suyehiro, 1986: Crustal structure across the Kurile Trench off southeastern Hokkaido by airgun-OBS profiling, *Geophys. J.R. astr. Soc.*, **86**, 371-397.

Stoffa, P.L., J.B. Diebold, and F. Wenzel, 1981: Direct mapping of seismic data to the domain of intercept time and ray parameter-A plane wave decomposition, *Geophysics*, **46**, 225-267.

Suyehiro, K., T. Kanazawa, A. Nishizawa, and H. Shimamura, 1985: Crustal structure beneath the inner trench slope of the Japan Trench, *Tectonophysics*, **112**, 155-191.

Suyehiro, K., T. Kanazawa, and H. Shimamura, 1986: Airgun-ocean bottom seismograph seismic structure across the Japan Trench area, in *Initial Reports of Deep Sea Drilling Projects*, Washington, D.C., **87**,751-755.

Tamano, T., T. Toba, and Y. Aoki, 1981: Trench slope survey of Japan Trench and Nankai Trough by reflection seismic method, *Butsuri-Tanko* (*Geophysical Exploration*), **34**, 38-55.

Yamada, T., 1980: Spacial distribution of microearthquakes and crustal structure in the subduction area revealed by ocean bottom seismographic observations, *Ph. D. thesis, The University of Tokyo* (in Japanese).